An assessment on effect of process parameters on pull force during pultrusion.

MUKHERJI, A. and NJUGUNA, J.

2022

AN ASSESSMENT ON EFFECT OF PROCESS PARAMETERS ON PULL FORCE DURING PULTRUSION

Arindam Mukherji[1,2] and James Njuguna[2,3]

[1]SP Advance Engineering Materials Pvt Ltd, SP Centre, 41/44, Minoo Desai Marg, Colaba, Mumbai. 400 005, India.

[2]Centre of Advanced Engineering Materials, School of Engineering, Robert Gordon University, Garthdee Road, Aberdeen, AB10 7GJ United Kingdom

[3]National Subsea Centre, 3 International Ave, Dyce, Aberdeen AB21 0BH, United Kingdom

Author to whom correspondence should be addressed; E-mail: j.njuguna@rgu.ac.uk; Tel.: +44 (0) 122 426 2304

Abstract

This research investigates the process behaviour by prediction of the pull force required to drag the raw materials through heated die at different reinforcing material configuration during pultrusion. Pultrusion is a continuous manufacturing process that is widely used in manufacture for composite profiles. A specially designed device, friction force by virtue of pulling on 'resin impregnated' fibres with both liquid resin and partially cured resin, was employed to measure pulling force against temperature and resin conversion. This allowed to experimentally simulate materials tracing in short and long die length used in process. Differential scanning calorimetry (DSC) was used to determining polymer conversion. The results shows that the downstream part of a die has no significant effect on the pulling force before certain conversion are achieved and that higher resin conversion leads to a higher friction at viscous /liquid zone. The difference is much more significant when the temperature is low (e.g., room temperature) and significantly drops due to on rising temperature. Mathematical model predicts increase in compaction pressure on increasing fibre volume fraction and drag velocity which is an opposite characteristic to tapping angle and part thickness considerations. Similarly, many parameters like shrinkage, viscous force and dry friction were modelled and simulated for ortho polyester resins as a function of temperature and resin conversion during dynamic pulling. The study has direct application in configuring pultrusion manufacturing customised for a specific configuring material, components manufacturing and respective designing of Die for the profile to be manufactured.

Keywords: - Pultrusion, Modelling, Die, Polyester, Curing, Compaction Force, Viscous Force, Frictional force, Drag Velocity

1. INTRODUCTION

The pulling of wet reinforcing fibres through die may simple however the dynamics and mechanisms of process parameters are very complex to fully comprehend due to continuous interaction between physical and chemical changes. Numerical and experimental investigations was attempted by several researchers to predict aspects of intrinsic pultrusion process to evaluate e.g. pressure [1–5], cure mechanism [6, 8], pull force [7,9,10] and heat transfer mechanism. Phenomena involved are mainly heat transfer controlling viscosity of the resin, resin conversion and phase changes, Die-material/surface in contact, and stress-strain behaviour. To model pultrusion process focusing pull forces, material inside Die is recommended to be divided into separate regions like taper region at wet material entry side, thermally active gel where process of curing is initiated, post gel region, and region of separation region or part detached from Die surface.

A statistical investigation on influence of process parameters like pull force and flexural strength of pultruded product was made by Lackey and Vaughan [11] and it was concluded that process parameters, influences pulling force, may vary significantly due to complex interaction change in cure kinetics. On the other hand, to have satisfactory experimental analysis, elevated number of variables involved are to consider, is an undesirable time consuming and money spending operation. Even prediction of part properties from process intricacy is barely perceptible. For any explicit understanding of pultrusion operation, mathematical modelling should embrace fundamental laws for heat transfer, conservation of mass and momentum. For simplification very few aspects are being studied, in providing numerical solution.

The process involves complex effect on cure kinetics resin, permeability, porosity, and shape factor of roving of reinforcing materials. The permeability of any porous material was first investigated and proposed by Henry Darcy widely known as Darcy's Law. Change in pressure gradients during flow for hydraulic fluid, depends on conductivity of the fluid involved wherein permeability and porosity controls pressure gradient for porous materials like resin impregnated fibres for thermoset and thermoplastics materials.

$$v = -K/\eta \nabla P \quad (1).$$

In the expression, v is the velocity of drag or pulling, K is permeability and ∇P is pressure difference and η is viscosity of resin. In Kozeny-Carman equation of permeability, where model for ellipsoid material with granular beds was assumed to be valid for fibrous porous media [12, 13] is widely used.

$$K = R^2/(4\,k_c) * [(1 - V_f)^3/{V_f}^2] \quad (2)$$

where k_c is the Kozeny constant, R the particle radius and V_f the fibre volume fraction.

Gutowski et al [61] analysed compressibility and permeability of carbon fibre stack impregnated with oil.

$$P = \frac{3\pi B\left(\sqrt{(V_f}/V_0)-1\right)}{[\beta^4\,(\sqrt{(V_a}/V_{f)}-1)^4]} \quad (3)$$

In the proposed mathematical expression P, is pressure normal to surface as given in eqn. (3) The transversal stiffness of fibres, B and β is the constant representing ratio of span length to span height of the fibres involved. Vf, final fibre volume fraction of the product wherein V_0 and V_a initial fibre volume and maximum fibre volume fraction re considered in the model. This expression is believed to be only pressure is being experienced by fibres packs.

In conventional pultrusion or in open bath pultrusion, compaction force or the pressure arises due to compaction is ignored due to low fibre volume fraction and short taper length. But with reasonable tape length in open bath pultrusion, increased fibre volume can be achieved without injection pressure [38-41]. Complexity of viscous region and compaction zone is profound for fast curing resin like polyester. Hence to maintain higher tapping and viscous length die, specific design is required to be adopted.

The analytical model of Kim et al [14,15] proposes pressure inside pultrusion die as unidirectional flow in pulling direction and zero permeability in z-direction. The expression is normally used for matrix continuity model.

$$dP/dx = U * \eta/K_{(x)} * [1 - V_{fx} - (1 - \Delta v/v)\ * (V_{fx}/V_f - V_{f(x)})] \quad (4)$$

In this eqn. (4), U is the pulling speed, $K(x)$ is the longitudinal permeability, and V_{fx} is the fibre volume fraction as functions of axial distance. $\Delta v/v$ represents the resin resultant volume change due to thermal expansion and overall shrinkage which can be ignore for simplification. Interactive pressure of respective regions can be calculated by Integrating this expression with elemental respective axial distance is expressed in eqn. (5)

$$P(x) = U * \eta/K(x) * [1 - V_{fx}/V_f] * x \quad (5)$$

However many researchers proposed injection pultrusion, total pulling force contribution is calculated as $F_{tot} = F_{com} + F_{vis} + F_{fric}$, where F_{tot} is total pulling force, F_{com} is compaction force and F_{fric} is frictional for after separation. These three different resistances are expressed separately by considering die width 'w' and axial distance:

$$F_{com} = = \int 2w(\dot{p} + \sigma) \tan\theta dx \quad (6)$$

$$F_{vis} = = \int 2w\tau dx \quad (7)$$

and

$$F_{fric} = = \int 2wf.\sigma\, dx \quad (8)$$

within $0 \leq x \leq x_{in}$.

Pull-force modelling for other injection pultrusion indicates that several factors like sliding induced shear, viscous adhesion force shrink induced part detached play's important role are unaccounted on analytical models. In eqn. (5) for compaction, eqn. (6) for viscous drag force and eqn. (8) of friction coefficient have neither considered thin layer resin at die composite interface for zones separately for Compaction Zone, Liquid Zones and dry profile zones beyond curing nor the thermal expansion and shrinkage. Even bending angle of reinforcing fibres as function of axial length in taper section which plays a major role in controlling pull-force is not conserved. Bending angle depends on the stiffness of the fibres and the length of the taper section die eventually compaction angle.

This work efforts are to capture complex variables like normal force, resin conversion, line speed, temperature by modifying many existing parameters during scale up operation. Pressure depending-variables are used in the proposed Model to predict the experimental results at operation. In this study, experimental quantification on pull force in compaction die are performed on conventional pultrusion Dies of two different tapping angles. wherein effect of temperature and fillers on straight die on friction is being testified by results received from inhouse made device. Along with polymer thin layer conversions separately for differ zones, Flat straight die profile, Thermal expansion and shrinkage, this mathematical model manifested the effects of Die-compaction angle, fibre volume fraction, thickness and drag velocity on pull-force. Therefore, aim of this paper is to evaluate the effect of process parameters on pull force configuring materials and designing of Die for the profile to be pultruded.

2. EXPERIMENTS

2.1.Materials

A continuous random glass fibre mats with 450 and 300 g/m2 (gsm) was provided by Skaps Industries India PVT Ltd. Owens Corning supplied glass roving used was of 4800 tex [tex: the mass in gram per one kilometre of a fibre roving]. A concoction of random glass mats and glass roving fibre package of 600 gsm were used. From SIGMA –ALDRICH Organically modified montmorillonite (MMT) which contains 0.05-5 wt% aminopropyltriethoxysilane and 15-35 wt% of ocatadecylamine, appearance (colour) white to off-white appearance (form) powder, loss on drying ≤ 3.0 %, Size ≤ 20-micron, density 200 - 500 kg/m3, (bulk density). Precipitated calcium carbonate (CaCO3) powder from Gulshan Polyols Limited, was employed as the conventional micron-filler of size ≤ 40-micron particle size. Orthphthalic acid based unsaturated polyester resin (MECHSTER™ 9000P) tailored for the pultrusion process from Mechamco was used in this study.

2.2.**Characterisation**

Differential Scanning Calorimetry (DSC) experiments were performed on a TA -60 Plus Shimadzu instrument, using hermetic pans and sample weights lower than 10 mg. The used materials in the experiments are formulated in resin paste and different low conversion as mentioned in Table1and 2.

Table 1

Isothermal scans were run at temperatures typically around 80ºC and kept it for 30 min to run out the residual Initiators. All curatives and additives are premixed separately before sampling. The sample preparation should be done swiftly in order to avoid loss volatiles like styrene results in loss of data during the first stages of the reaction. DSC determines the conversion of resin by measuring residual heat by thermal initiation. Table 2. Shows the final conversion and of curatives like Paradox-C, MEKP, BPO and TBPB used in the experiment.

Table 2

2.3.Pultrusion Line and Experiment set up

Working line Schematic used in our work is shown in Figure 1(a). The line consists of creel stands for roving and racks for felts, veil fabrics and unwinding continuous filament- mat (CFM), a resin tank, a pre-forming assembly composed of perforated steel plates and other guid rollers, a heated die, Die with heating elements along its length, a pulling unit and a flying cut-off saw. Temperature profiles along the die, pulling force, pulling speed, and pressure inside die are measured and recorded in data form. Hydraulic oil pressure exerted during pulling is monitored through PLC controlled pulling unit. This pultrusion pulling unit can either be used for open bath or closed die Pultrusion. In our regime Open Bath Pultrusion with 300 mm discontinued Tapping section used as shown in Figure 1(b).

Figure 1

Wetting of reinforcing fibres are very crucial for any composite part without dry patches. In open bath -Figure 1(b), impregnation, technique used to wet fibres is achieved by pulling fibres through resin tank. In order to ensure all fibres are sunk under resin, resin label is not allowed to go down below specified limit. Higher pulling speed and entangled fibres are avoided for better wettability. Impregnated fibres are guided through guide rollers and plate and finally through preforming assemble to have specified part cross section prior to entire into Die. When pulled through the resin bath, excess of resin carried by roving at die entry, will wet-out cloths like polyester veil or glass veil. Discontinued compaction tapper section assists in squeezing out Excess resin and trapped air to get void free pultruded parts (typically between 1 and 5% vol.) can be produced. Curing to solidification of profile is made by passing the squeezed material through heated Die. Die Temperature management is crucial in order to produce good quality components, hence a gradual increase in resin temperature is achieved by placing more heating zones with different set temperatures along the length of the die Time of mat entry during travelling though die, was recorded by the thermal sensors placed between the fibre pack. The fibre-package consisted of 10 layers of Bidirectional mats with 600 g/m^2 and 60 roving with 4800 tex. The thickness of the produced composites was 8 mm. of high-pressure tapper die, Figure 1(b).

Many variations on trials were conducted on adding additional mats, on the high-pressure conventional dies. Add-on reinforcing method in pultrusion is used to find pull force throughout the die used at different speed and filler loading, the temperature at surface and core during pulling is also recorded. To trace the magnitude of pull-force change, additional mats, 200 mm wide and 254mm long, were inserted in the centre prevailing fibre pack. The speed of pulling was set at 20-50 mm/min. Thermocouples were placed in between the mats to measure the temperatures of core and surface as well. The pulling speed was set at different speeds like 20 mm/min and 45 mm/min. As the mats travelled through the die, the time mat entered the die was recorded and based on speed, axial distance is calculated against pressure appeared. The experimental result for the high-pressure conventional die with extra tapping section is shown in Figure 1(b) x-axis, pulling force magnitude positions front edge of the additional mats traveling along the die and y-axis, pulling force magnitude positions die-centre towards wall Pulling is recorded separately for each driving forces which governs the ultimate pull forces.

In addon reinforcement in running operation was conducted in conventional Die with discontinued specially designed 0.3 metre Tapper section as shown in Figure 1(b). As Compaction zone is predominating on other frictional forces, separate experiment for downstream part of the die which undergoes resin drag and dynamic friction before gelling are required to conduct at room temperature. A short length and long length die without tapper portion were used to comprehend contribution of friction of viscous zone and influence of its subsequent length. Further, influence of die length on pulling force was investigated using different Die lengths. 1200mm, 800 mm and 500 mm three conventional dies were employed in this experiment. The pulling speed and the fibre package remained unchanged as used in addon reinforcing Method. Schematic of the experiments in short die and long Die are shown on Figure 2(a) and (b). All along ‘Low fibre volume fraction’ were maintained in short and long dies.

Pull force arises from friction between composite and the die surface predicts the effect of Temperature, Resin conversion, pulling speed at gelling and post Gelling region. anticipating shrinkage and thermal expansion of the product.

Figure 2

As shrinkage coefficient is governed by conversion of polymers and the filler loading in resin. Composites with different shrinkage factors were considered in conducting trials. The short 500 mm single cavity die as mould was used to find the compressive stress during compaction at different thickness and steel shim placed beforehand in the die was pulled to record pulling force against time for straight portion at different temperature, resin conversion and pulling speed. Compressive stress and pulling force required was recorded by an Instron universal testing machine (Model -Delta -C200 -10 Tons) attached. The side-view of the mould is also shown on Figure 2(a) and (b). Experiments were conducted on the same short die but keeping length of the steel plate long. Arrangement is made in such a way the plate is three times longer than the mould to keep the contact area constant throughout the experiment. The experiment was conducted for three different filler loading in a resin of specific shrinkage factor, for two resins of different shrinkage factor at 105 °C constant temperature. In the experiment the plate was wrapped with resin impregnated glass fibres at different % conversion.

The resin was formulated to have different % conversion and steel plate was pulled for a span of 6 mins at speed of 10 mm / min. Formulated resin as listed in Table 1 was used in impregnating reinforcing materials and two layers of random mats with surface veils used for wrapping steel plate. Percentage conversion is controlled by placing reinforcing materials in a preheated 90 °C mould with specific thickness, and maintained heating for 30 min. The heated plates for the that period is long enough to run out the initiators from Parkadox based formulated resin system. Different % conversion was confirmed by the DSC before keeping on the single cavity mould holding amid the steel shim. The mould was completely closed and pulling test was performed in three different stages. In First stage, steel plate was pulled out by one-third of the total length at room temperature followed by 60 °C and 105 °C for remaining subsequent shim length. All along 200 mm/min pulling speed was maintained and pulling force due to friction is recorded. Several impregnated partially cured fibre mats were first wrapped by surface veils as used in actual pultrusion process, then laid up evenly in both mould halves. A chromed steel shim of 2.0 mm in thickness and 90 mm in width and 300mm length was placed between the fibre reinforcement materials, and the mould was closed. The dimension of the mould cavity is 8mm thick, 100 mm long, and 100mm wide - the initial contact length of the plate and the fibre mats is 100 mm, thus the initial contact area of 90 mm by 100 mm. To prevent fibres from moving up during pulling high fibre volume fraction was maintained providing a high holding force.

Steel plate out of the mould at a constant speed was pulled gradually and force change versus time was recorded by Instron universal testing machine tester. From known cross sectional

area, pressure can be calculated wherein friction of coefficient obtained is pulling force divided by the contact area and the compaction stress. In investigating temperature effect on friction, heating tape is used on steel slim, wherein change in temperature is monitored. Liquid region friction experiments at different temperature were carried out by wrapping prepreg with different % conversion on steel plate placed into the mould as described in pultrusion operation. Similarly, material described in pultrusion method, resin with different filler contents like 10, 30, and 40 phr, were used.

3. RESULTS AND DISCUSSION

3.1.Pull force Modelling.

The pressure accounts force due to compaction at tapping Zone, friction due to viscous Drag and Friction due to cured product with Die surface. The modelling and simulation are strongly dependent on many physical process variables which needs to be investigated. Many Models are being available like Thermo-chemical modelling, Fluid dynamics modelling, Thermo-mechanical modelling etc to investigate behaviour change in pressure being experienced by the fibre pack during pulling through die. Three pressure that fibre pack being experiencing mainly during drag are compaction resistance, Viscous resistance, and friction resistance (dry fibres and solid profiles with Die Surfaces).

Compaction resistance are mainly due to resistance of fibre bed to get squeezed during compaction depending on fibre volume fraction influenced by Porosity of fibres and Permeability of resin [15-22].

$$\delta = F * L^3/(192E * I) \quad (9)$$

$$L = \beta * (l_0 - l_{min}) \quad (10)$$

$$\delta = (l_0 - l) \quad (11)$$

Assuming $l_{min} = d$,

$$P = F/L * w = [(l_0 - l)192 * E * I]/\beta * (l_0 - d)^3 \dot{w} \quad (12)$$

B *is* Bending stiffness $= 192 * E * I$, (13)

considering , $\dot{w} = L$,

$$V_f = \pi d^2/4l^2, \quad (14)$$

$$V_0 = \pi d^2/4{l_0}^2, \quad (15)$$

$$V_a = \pi/4, \quad (16)$$

where *'L' is* length of the Fibre Segment, *'E' is* Modulus of the Fibres, *'d' is* diameter of the fibre, *'I' is* Inertia of Bending of the Fibres, *'F'* is Contact force of the Fibres, *'l_0'* is Initial height of the prism, *'l_{min}' is* Minimal Height, *'l'* is height, *'β' is* Constant by microscope span height to span length ration of fibres network, *B is* Bending stiffness.

$$P = 3\pi B\,[\sqrt{}\,(V_f\,(x)/\,V_0) - 1]/\,\beta^4[\sqrt{}\,(V_a\,/\,V_f\,(x)) - 1]^4 \quad (17)$$

This was modified by Gutowski's formulation [17] for compaction zone with index $\hat{n}$=2. By principle of porosity in conical Die,

$$\{V_f\ (x)\} = (h_L * V_f\ )/[\,h_L + (L_m - x) * tan\,\theta] \quad (18)$$

$$P = (3\pi B/\sqrt{\varepsilon})\,[\sqrt{}\,(V_f\,/\,V_0) - \sqrt{\varepsilon}]/\,\beta^4[\sqrt{}\,(V_a\ * \varepsilon\,/V_f) - 1]^2,$$

Where $\varepsilon = 1 + 2(L_m\ - x)/\,h_L\,tan\,\theta$ (19)

Fibre volume fraction can be calculated by deciding N_r (No of Roving in any Particular Volume). Where N_r is the number of roving used in the specific volume and L_w is the linear weight of fibre. Final volume fraction of um-reinforcing material [11,12,14] is a quantitative value of porosity(*Φ)*, i.e. $(1 - V_f) = \Phi$, and permeability (*K*) as proposed by Henry Darcy is

$$V_f = N_r \cdot * L_w/\,(A * \rho_f) \quad (20)$$

Theoretical values used in Model fitting of $V_0 = 0.350, V_a = 0.785$ square and 0.907 for hexagonal, $\beta = 2.54 * I = 2.61 * 10(-7)\,, E = 8.2 * 1010,\ \rho_f = 2620\ kg/m2, L_w =$ 4800 $[tex]$ for glass,

$$\int dP_f = \int\ (3\pi B/\sqrt{\varepsilon})\,[\sqrt{}\,(V_f\,/\,V_0) - \sqrt{\varepsilon}]/\,\beta^4[\sqrt{}\,(V_a\ *\ \varepsilon\,/\,V_f) - 1]^{\,2}dx \quad (21)$$

This is the pressure experienced by fibre beds not by the resin or matrix. Hence compaction pressure on matrix is evaluated.

$$U_x = (K/\,\eta)\ *\ \delta P, \quad (22)$$

where U_x is the resin flow speed, *K* is the permeability and η is the resin viscosity, δP is the pressure gradient and Permeability by Kozeny-Carman [19],

$$K = d^2\,(1 - V_f)^3\,/Kc * {V_f}^2 \quad (23)$$

From Fibre continuity,

$$V_f\,(x) *\ h(x)\ =\ V_f\ *\ h_L, \quad (24)$$

Since, $[h_L/\,h(x)]\ =\ (V_f\,/\,V_0)\ + (1 -\ V_f/\,V_0)\,x/L_m$ (25)

$$V_f\,(x) =\ V_f\,/[\,(V_f\,/\,V_0)\ + (1 -\ V_f\,/\,V_0)\,x/L_m], \quad (26)$$

From matrix continuity [20,21] on volumetric flux,

$$Q(x).h(x) = U_x\,(1 - V_f) * h_L, Q(x) = U_x\,[(V_f\,(x)/V_f) - V_f\,(x)] \quad (27)$$

Relative matrix flux

$$Q_R(x) = [Q(x) - U_x\,(1 - V_f(x))] = U_x\,[(V_f\,(x)/V_f) - 1] \quad (28)$$

Since apparent viscosity of the Carreau model may be written

$$\eta_a = \eta_0\,(1 + (\lambda * \gamma)^2)^{(n-1)/2} \quad (29)$$

From Darcy equation, $P = (U_x * \eta)/K$,

$$(dP/dx) = [Q_R(x) * \eta]/K \quad (30)$$

$$(dP/dx) = Q_R(x) * \eta_0(1 + (\lambda * \gamma)^2)^{(n-1)/2}]/K, \quad (31)$$

γ = shear rate or velocity divided by layer distance,

$$dP/dx = \frac{[Q_R(x) * Kc * V_f(x)^2 * \eta_0[1 + (\lambda * \gamma)^2)^{(n-1)/2}]}{d^2\,(1 - V_f\,(x))^3} \quad (32)$$

By principle of porosity in conical Die,

$$\{V_f\,(x)\} = (h_L * V_f\,)/[\,h_L + (L_m - x)\,tan\,\theta] \quad (33)$$

Now as per pressure Gradient by Darcy's Law [5,7,19],

$$dP/dx = \int dP_d$$

$$= \int \frac{G \cdot \eta \cdot U \cdot {V_f}^2 \cdot {h_L}^2\,.(L_m - x)\,tan\,\theta}{d^2 * [(1 - V_f)\,h_L + 2(L_m - x)\,tan\theta]^3}\,dx \quad (34)$$

where Gebart, defined shape factor G, as 57 for a quadratic fibre arrangement [23,24]. Since P_d is pressure due to drag, would be considered only because of matrix and for fibres bed reacting is the P_f, Hence Compaction Pressure is a combined effect of matrix and the fibre bearing load. Compaction resistance is predominantly influenced by taping Angle, fibre Volume fraction speed of pulling and part thickness. In predicting resistance initial taping angles θ radian is potentially considered for models but principally taping angle varies with axial distance which needs to be considered for fibre beds. Fibres close to core are experiencing less bending compared to fibres close to surface. Hence in this study, 'θ_f' an average angle was calculated considering the gradient of change in taping angle depends on length of compaction zone and shape factor of reinforcement.

$$R = \int (\theta - 1.47 * Z.^3), 0.000 < Z < 0.25), \theta_f = (R./0.25) \quad (35)$$

$$\int dP_c = \int P_f \, Cos\, \theta_f \; * \; sin\, \theta_f \; dx + \int P_d \, sin\, \theta_f \; dx \qquad (36)$$

Viscous resistance is believed to be drag resistance influenced by viscosity of resin and drag speed. Viscosity is a direct implication of the shear stress on composite surface before complete curing between gelling and post gelling phase [22-27].

$$\int dP_v = \int (\eta_a U/r \, Cos\, \hat{\theta}\, dx \qquad (37)$$

$$\int dP_v = \int ((\eta_0 \, (1 + \, (\lambda * \gamma)^2)^{(n-1)/2}) \, U/r \; * \; Cos\, \dot{\hat{\theta}}\, dx \qquad (38)$$

r is the distance between the layers or fibres, varies with fibre arrangement [7,23,27] like

$$r = d \, (1 - \sqrt{} \, ((\sqrt{3}) \, (\pi \, V_f \, (x))/2)/2) \qquad (39)$$

But in our study adhesion of resin layer to the surface of die plays additional roles and is influenced by increase speed lessens heat effect on viscosity of resin. (stress * gradient of speed) $Cos\, \dot{\hat{\theta}}$ was called liquid-solid affinity, where $\dot{\hat{\theta}}$was contact angle of liquid-solid phase and σL was interfacial surface tension of solid-slurry. infiltration and permeation ability of the liquid resin is directly influenced by affinity of the liquid and higher adhesion force. Policed Die Surface decreases affinity between liquid resin and solid die surface. As viscosity changes with time influenced by heat, average viscosity was considered in our study.

Considering the initial practical viscosity of the resin used is 0.4 Pa.s, average viscosity,

$$\int d\, \eta_v = \int (0.4 * exp(.0894 * t)\, dt, \qquad (40)$$

$$0 < t < (x - L)/U$$

adhesion load,

$$\int dA_d = (520 - (0.025 * (\eta_v / (x - L_{\mathrm{m}})/U)) * 2 * 3.14 * h \qquad (41)$$

$$\int dP_v = \int (\eta_0 \, (1 + \, (\lambda * \, U/r)^2)(n-1)/2U/r) * \, Cos\, \dot{\hat{\theta}} dx$$
$$+ \int (520 - (0.025 * \, \eta_v \, / (x - L_{\mathrm{m}})/U)) * 2 * 3.14 * h_L \, dx \qquad (42)$$

Friction resistance arises from Dry fibres and solid profile with die surface.

$$\int dP_f = \int Pd\, (x) * f * Cos^2\, \theta\, (x))\, dx \qquad (43)$$

where *f* is the friction coefficient. When the surface of the composite is solid, the expression is considered as normal stress between composite and die.

In our study, pull force model for friction resistance, shrinkage induced part detached pressure which plays additional role to reduce friction is considered. Hence the existing normal stress between Die and solid profile gets reduced by $(\hat{G}\,\delta R/r)$ helping to get part detached. Theoretical Bulk Modulus of the resin is $\hat{G} = 4.* 10\text{^} (8)$, *and* $0.75 < x, 1.5)$, [4,5,20] *Wherein* G-Bulk Modulus, δR -shrinkage of resin and $\hat{\lambda}$- resin layer thickness. δR is the shrinkage of part which we can assumed as change in length as radius parameters like shrinkage factor (S) of the resin, layer thickness $(\hat{\lambda})$ and extent of curing controls normal stress as modified to

$$\int dP = \int (\hat{G}).* (r)/(0.2 * (x))dx \quad (44)$$

$$\int dP_{ef} = 0.085 * \int dP_f - \int dP \quad (45)$$

3.2.Start-up Experiments and Slip Phenomenon

As shown on Figure 3, during start-up stage, two different situations are analysed. One where reinforcing fibre saturated with only pristine resin and another wherein resin contains 30phr filler and 5.5 phr nanofillers are pulled through the Conventional 'Open Bath' discontinued tapper Die, maintaining 50 mm/min pulling speed. The pulling force trajectory against times of Figure 3., shows that dry fibre package pulling pressure reaches to maximum at 625 sec and leads to 5398 N force but after about 650s as pure resin began to run out, pressure drops and leads to 3429 N force for a specific area Die Profile. The shoulder of decrement observed faster for 30Phr filler loading in respect to 5 phr MMT treated Nano filler This experiment indicates that friction is more for wet fibres with Nano fillers but more vulnerable for dry fibres. The probable explanation could be due to interface layer thickness of resin which minimises the friction between fibres and die wall. Thicker the layer of resin as in case of higher viscosity due to higher filler content and less, as expected for pure resin and low dosed nano fillers, less would be the friction in between reinforcing fibres and die wall. Fillers are an essential component in the resin formulation which must be configured to have corrosion and heat resistance with good surface finish at low cost.

Figure 3

3.3.Compaction Effect by Addon Reinforcement

Unlike the analytical and simulation model [43] shows sudden rise in pressure rise from 0-bar to 160- bar and then gets plateau in our case, initially as the addon Reinforcement travels through die as shown in Figure 4, pull force trajectory remained unchanged untill 100 mm but follows sinusoidal pattern to reach maximum value (4680 N) and gets stabilised subsequent of gradual decrease in pressure. This sinusoidal trend of increasing of peak and resuming original value are noticed as fibre pack travel moves down axial distance. Indeed, peak gets broaden followed by gradual increase at initial compaction and drops insidiously till tapping angle gets flattened but hardly any change is observed in overall pulling force, for additional reinforcement.

Figure 4

Temperature change near the surface and inside the composite, is recorded by thermocouples placed in the fibre package, one at just beneath the surface veil and another in the middle of fibre package. It is observed, rise in temperature is barely perceptible till the compaction zone ends, but interestingly, temperature change caused by the exothermic resin reaction just before 300mm away of exist end, reached its maximum value. This implies that rest of the pulling force develops in late stream zone is due in the gelling effect and solid friction post- curing. This implies composite cohesive force gets debilitated to die surface facilitating loose contact before the reaction peak temperature.

Figure 5

Unlike simulation model [43] that shows rise in pressure rise observes after traveling certain axial distance of 300 mm die inlet wherein in our case as observed in Figure 5, right from die entry with decreasing compaction taping angle, magnitude of pull force increases and vice versa. The peak observed at entrance flat portion of die which experiences major compaction. Again, the late stream part of the die has less responded to the additional mats, but fliting response pattern observed with decreasing tapping slope.

Figure 6. shows the similar trend in increases of Pulling force with increasing pulling speed from 0.2 to 0.45m/min. Responds to pull force is higher and sensitive to higher speed similar to studies found in [43] wherein pressure increased from 0-80 and 0-68 bars for higher and lower speed with similar tapping angle. A possible explanation is initial pull force is the existing pull forces and for any additional reinforcement at compaction experiences more

pressure to accommodate the solid reinforcement into final die gap squishing out excess viscous resin. Viscous drag forces mainly late stream part of the die contributes marginally unlike compaction forces of total pulling force [6,7,25,28].

Figure 6

Hence, of a good understanding parameters in scale up operation to get stable product (Figure 7 (a).) are crucial otherwise one may encounter problems like over curing of the parts and eventually loss of heat, warpages of the product due to uneven curing, low productivity due to slow pulling speeds, scaling at part edge (Figure 7 b and c.), seizure of dies and ultimately line/part failure (Figure 7 d.), higher pulling force required leads to higher electrical (energy) consumption during manufacturing stage.

Figure 7

In our study MATLAB software was employed considering other influencing parameters like fibre volume Factor, tapping angle of Die, thickness of the profile and drag velocity is computed in Model fitting simulating experiments results. It was found, model is in good agreement with degree of compaction as recorded experimentally. It is worthy to mention, we are restricting axial length separately for compaction from 0 to 0.3m where in for 0.3 to 1.5m for flat portion for pressure due to Viscous and Friction. From model fitted 2D Graphs, paradigm of compaction pressure changes with sweeping Fibre volume fraction, drag speed and profile Thickness as appeared are similar to recorded experimental results but rising trajectory are sharp, prominent and clear. In model fitting, variables like tapping angle ranges from (0.014 to o.019^{o} Radian), Fibre Volume Fraction varied from (0.480 to 0.620), Part Thickness ranges from (0.004-014 Mt) and Drag Speed varied from (0.0020-.0032 M/s).

Figure 8

Using the governing eqn.36 as derived from eqn. (9-35), compaction pressure is plotted against many complex variables. It is found that tapping angle has negative influence on pressure which shows sensitive to higher values of variables when plotted in 2D graphs as shown in Figure 8 (a and b). Pull-force appeared sharp increase and lasts longer for thick profile but drops insidiously unlike thin profile, wherein sudden drops in pressure observed of parameters

like fibre volume fraction and speed of pulling. with increasing speed and tapping angle, change in pulling pressure is plotted. Similarly, as shown in Figure 9 (a and b), increased pull-force is perceptible profoundly for increasing velocity, but difference is barely perceptible for dropping pressure, wherein for increased tapping angle shows long lasting pressure along axial distance.

Figure 9

3D-surface plotting as shown in Figure10 (a). depicts nature of Pressure drops swiping thickness as functional parameters long axial distance. Spikes appeared prominently sharp and profound for ‘Higher speed’ and ‘tapping angle’ deviating shifting harmony in axial distance. Similarly, Figure10(b), depicts paradigm of increased pressure swapping speed of Pulling or Drag velocity as function maintaining shifting harmony in axial distance. A comparison between measure values with Model fitting is elicited in table 2.

Figure 10

Table 3.

3.4.Viscous force Phenomena in liquid Phase

To explicit the contribution experiment was conducted to investigate the contribution of viscous drag force to total pulling force. As shown in Figure 11, pulling force at 80 mm/min speed, both dies (450 mm and 960mm) dies show no significant change at liquid phase. Hence increased length of straight portion in die makes no difference with shorten die length unless viscosity gets influenced by temperature, pulling speed and fibre volume faction. Before gelling as indicated in the addon reinforcement method the pultrusion die does not contribute significantly to the pulling force, similarly predominantly in liquid phase, straight portion of longer die length cause no increase is pulling force. Pulling force in this region only due to reaction stimulated gelling and post gelling resin until the surface solidification.

Figure 11

3.5.Viscous force verified by steel-shim

A thin liquid layer exists between fibres and the die surface in the liquid zone have been assumed in the literature [29,30] is controlling factor of pull force and increases with increasing pulling speed or assumed proportional to overall pulling force. The phenomena are witnessed by compaction and viscous zone irrespective on influence of temperature.

The concoction behaviour resin gelling from liquid and subsequently to solid during operation through pultrusion die is very deceptive to comprehend. Viscosity gets burgeoned rapidly on gelling of resin, due to viscous friction at die surface. At die-composite interface, such mechanism of viscous friction could be influenced by resin conversion and temperature. Hence it is intrigued to investigate the influences of processing parameters on friction force. A short length die with steel plate, were used to comprehend influence of temperature, conversion, filler loading of resin on friction of viscous zone. In experiments, heating tape wrapped around steel plate placed inside short die equipped with temperature controller, to facilitates to have different temperatures as described above. Process of controlling % conversion of resin and testifying the same by DSC was discussed above. In friction measurement process, different final conversion is achieved by adjusting reaction temperature, reaction time and amount of low temperature initiator (MEKP) [31-32,38-41]. Perkadox-C is also a low temperature promoter which synergise the influence of MEKP at a particular temperature. Benzol peroxide (BPO) a initiator is mixed with promoters Tertiary Butyl Per-Benzoate (TBBP) to have conversion at higher temperature.

The friction is the direct implication of pull force and can be measured as function of both parameters' temperature and resin conversion. The stress normal to die surface is recorded by the pressure transducer. Pulling force required to pull thin plate is comparatively low but it is reasonable to compare pressure. There are initial drops in pressure due to drops in viscosity, but tension starts rising with passing secs. The most probable explanation would be due to shear thinning due to heat and shear effect of unreacted polymers and monomers facilitating pull force to decreased greatly [26-28]. which may further be influenced by increasing speed. Further in the event of different % conversion at different temperatures, nature in changing friction and stress inside during viscous drag at Gel and post Gelling region is shown in Figure12. Pull-force for 30 % conversion recorded at room temperature (25 °C) is higher

compared that at 60 °C, wherein difference is more profound at 50 % conversion resin impregnated fibres. This indicates that friction due to viscous drag becomes larger when resin is at ‘Gel State’ and with increasing temperature at any given constant contact pressure situation gets more vulnerable for higher molecular weight resin. As the matrix starts crosslinking, affinity to die surface gets lessen and eventually reduces adhesion force is presumed but increasing viscosity increase pulling force in viscous phase. Overall trend implies, higher temperature promotes crosslinking more keep the resin viscous more to a maximum extent, compare to low temperature.

Figure 12

Similar using governing eqn.42 as derived from eqn. (37-41) and subsequent model fitting by using MATLAB software considering parameters like drag velocity, Fibre Volume Fraction, thickness of the Profile and tapping angle, simulation was computed to compare experiments results. In our study, adhesion force is considered which contributes significantly at low surface tension between solid and liquid surface interface. The surface tension directly varies with viscosity and that varies with speed. As drag speed increases, contribution of adhesion force to total Viscous force is less significant. Hence average viscosity was taken during fibre pack travel in flat Section. 2D-Plot as shown in Figure 13(a), it is found that viscos pressure responds promptly with increased Drag velocity wherein in Figure 13(b), similar behaviour as observed in compaction pressure, pressure shows decremental with increasing tapping angle. Figure 14(a and b) for change in profile thickness and Fibre Volume Fraction, show similar paradigm as observed in compaction, but the overall contribution to total force is less. It is worthy to mention, axial length is restricted to 1.5m for flat portion. From model its evident that paradigm is incremental and tends plateau due to increase in viscosity leads to gelling and subsequently to solidification. Gelation process is much faster and abrupt at higher temperatures and after gelation, the curing continues with much slower pace because of the restricted movement of reactive groups. It worthy to mention that gelation effect at faster heating rate causes the reaction rate, a diffusion controlled. This limited diffusion causes seldom failure to reach the complete conversion. Gelation time is accurately determined from half-life and the time required to reach the maximum cure rate as normally calculated by isothermal cure kinetics of unsaturated polyester resin.

Figure 13

Figure 14

3.6.Dynamic friction force after cure

Separately using governing eqn.45 as modified of eqn. (43and 44) and subsequent model fitting by using MATLAB was made to investigate post curing Solid surface friction of product. In the Governing equation, shrinkage induced part detached is considered. In order to rule-out undesirable uncured fibre pack core of thick part, alongside an experiment of steel shim pulling, conducted in short die length. The results recorded may not in line with exactly with 2D plotted model fitting for Solid surface friction. Experiment using same short die with heated steel shim is conducted to predict the pulling force beyond curing at profile at Die surface. The device which has better control on speeds of pulling and temperature plate can have better accuracy to understand behaviour of pull force beyond curing. This long-cured zone, pulling is mostly generated due to dynamic friction of composite in contact with die surface.

Figure 15

Dynamic dry friction on different resins with specific shrinkage factor during pulling was recorded at 105^{o}C as shown in Figure 15. During the period of dry pulling, with Initial drops, friction gets stabilised with time. In addition, it is observed, with time a steady state appeared at marginally higher value of friction in the event of low shrinkage resin. Similarly effect of filler and % conversion on friction during dry drag was studied as shown in Figure 16, With initial drops, friction embarks slow rising for all variants. Reason of nitial drops is not understood clearly but increasing filler amount like 40% to the subsequent 30% and 10%, shows incremental rising trend.

Figure 16

Beyond curing, comparatively higher cohesive force between die wall and matrix for resin at low filler content resin opposite for higher filler loading [29-32,34,35]. The initial drop may be explained as higher filler loading increase matrix morphology stiff and thereby reduces the dynamic frictional coefficient but with passing time, all variants get stabilised with higher

friction at higher filler content. Further addition of filler makes the resin thicker, and rate of reaction slows down, and diffusion phenomena is more predominant which may delay conversion starts playing in due to heat on resin layer due to higher viscous resin, in die interface ultimately decreased stress compressibility.

Similarly, two different conversion of same resin was used to predict the behaviour of dynamic friction of the composite beyond curing. The reason of slightly higher pull force for resin at higher conversion, at start is not clearly understood. But apparently higher molecular network restricts to slip initially [33] but stimulate sliding on curing faster than resin at low conversion, reducing contact stress with time. Pulling force gets stabiles with time and difference between low and higher conversion is barely perceptible.

Figure 17

Unlike experiments pulling force in 2D plot sweeping time, axial length is sweeping against pulling pressure. However, drops in pull-pressure is evident in resin with Higher shrinkage factor due to increasing negative pressure on total pressure of solid friction. The paradigm of pressure drop is very steady, almost similar pattern and consistent as is observed in 2D-Plot shown in Figure 17 (a and b) and 18(a). As found for compaction and vicious, increase in tapping angle has negative influence on Frictional pressure wherein thickness and Fibre Volume Fraction and positive influence. The gradual and steady drops pressure with increasing resin shrinkage factor is perceptible on minimising scale of pressure axis as plotted in Figure 18(b). It can be concluded that increasing part thickness and Fibre Volume Fraction, increase Pressure due to Frictional. Amount of pressure goes up exponentially with increasing thickness and Fibre Volume Fraction and wherein pressure drops is noticeable severely for change in shrinkage factor.

Figure 18

4. CONCLUSION

Current studies revel pulling in open bath pultrusion pulling pressure certain for any cross-section encounters associated frictional force which gets influenced by many crucial

parameters like Die Tapping Angle, Die Radius, Thickness and Length of Die, Die Surface Smoothness, Guiders and Resin Tank used, Heater position from Die entry, Die temperature, Pulling speed, Fibre volume fraction, Configuration of material at die interface, Resin viscosity, Resin releasing rate from reinforced fibre, Size and Porosity of Filler and its Loading percentage. Even though it is difficult to develop model which predicts paradigm of burgeoning pull-force during large scale operation, the proposed modified Mathematical equation enables one to comprehend effect of intricate process parameters on pull force measured and its fitting in the Model. Pressure arises at compaction zone is always predominant over pressures like viscous drags and dynamic friction.

Results show that during viscous phase, higher resin conversion leads to a higher friction and unlike speed of pulling, viscous friction is much more significant when the low temperature (e.g., room temperature) wherein friction drops at higher temperature and eventually debilitated at solidification. Again, it is found that Die seizure/sloughing leads to fibre breakage is appeared mostly in case of smaller die due to surging adhesive force between die surface and resin, can be mitigated by using mould releasing agents. Hence sustainability of smooth operation during pulling relies on ultimate tensile strength of the part rather strength of the fibres being pulled in machine direction. On the other hand, gelling and post curing solidification cause significant spikes in the pulling force on enlarging die length. But longer dies in pultrusion benefits in maintaining good dimensional stability against heat distortion should not be ruled out. Again it is worthwhile to mention, pull-force measurement alone is not a satisfactory indicator of part curing at the exit and experimental verification on residence time, distribution heat and surface cure at the exit are required to substantiate at pulling operation.

DECLARATIONS

a. Funding

The authors are thankful to financial support for AM from Shapoorji Pallonji Group through secondment to Robert Gordon University for a Research Fellowship in a project titled ‘Honeycomb Composite Structures for Ballistic Protection’ Project No. 120437.

b. Conflicts of interest

The authors have no conflicts of interest to declare that are relevant to the content of this article.

c. Availability of data and material
The image data used will be provided on request.

d. Code availability (software application or custom code)
The code used will be provided on request.

e. Ethics approval
The authors declare no competing interests.

f. Consent to participate (include appropriate statements)
N/A.

g. Consent for publication (include appropriate statements)
N/A

h. Authors' contributions
AM**:** Conceptualization, Investigation, Methodology, Writing - Original Draft, Writing - Review & Editing, Validation, Funding Acquisition. JN**:** Conceptualization, Methodology, Writing - Review & Editing, Project Administration, Resources, Funding Acquisition Supervision.

REFERENCES

1. I. Baran, C. C. Tutum, and J. H. Hattel (2013). The effect of thermal contact resistance on the thermosetting pultrusion process. Composites B, vol. 95, pp. 995–1000.

2. Batch, G. L, & Macosko, C. W. (1990). Analysis of pressure, pulling force, and sloughing in pultrusion. American Society of Mechanical Engineers, Heat Transfer Division, (Publication) HTD, 132, 109-112.

3. Struzziero G , , Maistros G.M , Hartley J, Skordos A. A (2021). Materials modelling and process simulation of the pultrusion of curved parts G. Composites Part A 144 106328.

4. Baran, C. Tutum C., Nielsen M.W, and Hattel J. H. (2013). Process induced residual stresses and distortions in pultrusion. Composites B, vol. 51, pp. 148–161.

5. Dong C. (2009). Modeling the process-induced dimensional variations of general curved composite components and assemblies. Composites A, vol. 40, no. 8, pp. 1210–1216,

6. Gorthala R., Roux J. A and Vaughan J G. (1994). A Model to Predict Resin Pressure/Back Flow in the Tapered Inlet of a Pultrusion Die, Journal of Reinforced Plastics and Composites, Vol. 13-June

7. Astrom B. T (1993). Modeling Approach to Thermoplastic Pultrusion. I: Formulation of Models, Polymer Composites. Vol. 14, No. 3

8. Rahatekar S. S. (2005). Injection Pultrusion Simulation for Polyester/Glass Mat/Rovings/Mat Composites. Journal of Reinforced Plastics and Composites, vol. 24, no. 1, p. 53–68.

9. Baran I., Hattel J. H., Akkerman R. and Tutum C. C. (2015). Mechanical Modelling of Pultrusion Process. Applied Composite Materials, vol. 22, no. 1, p. 99–118.

10. Vernet N. et al (2014). Experimental determination of the permeability of engineering textiles: Benchmark II. Composites Part A: Applied Science and Manufacturing, vol. 61, pp. 172-184.

11. Lackey E. and Vaughan J. G. (1994). An analysis of factors affecting pull force for the pultrusion of graphite/epoxy composites. Journal of Reinforced Plastics and Composites, vol. 13, no. 3, pp. 188–198.

12. Josiasvd W, J. Prieur Du P (1994).Quantification of Unidirectional Fiber Bed Permeability," Journal of Composite Materials, vol. 28, no. 7, pp. 619-637

13. Bates P. J, Taylor D and Cunningham M. (2000). Transverse Permeability of Direct Glass Rovings. Journal of Reinforced Plastics and Composites, vol. 19, no. 15, pp. 1217-1226.

14. Kim D.H, Han P.-G, Jin G H. and Lee W. I. (1997). A Model for Thermosetting Composite Pultrusion Process. Journal of Composite Materials, vol. 31 (20), pp. 2105-2122.

15. JOSHI S. and LAM. Y (2006). Integrated approach for modelling cure and crystallization kinetics of different polymers in 3D pultrusion simulation. Journal of Materials Processing Technology, vol. 174, no. 1-3, pp. 178-182.

16. Baran I, Akkerman R and. Hattel J. H (2014). Modelling the pultrusion process of an industrial L-shaped composite profile. Composite Structures, vol. 118, p. 37–48.

17. Carlone P, Palazzo G and Pasquino R (2006). Pultrusion manufacturing process development by computational modelling and methods. Mathematical and Computer Modelling, vol. 44, no. 7-8, pp. 701-709.

18. Baran I, Hattel J. H, Tutum C C and Akkerman R (2015). Pultrusion of a vertical axis wind turbine blade. part-II. International Journal of Material Forming, vol. 8, no. 3, p. 367–378.

19. Carlone P., Baran I, Hattel J. H and. Palazzo G. S (2013). Computational Approaches for Modeling the Multiphysics in Pultrusion Process. Advances in Mechanical Engineering. vol. 5, no. 0, p. 301875.

20. Baran I, Hattel J. H and Akkerman R (2015). Investigation of process induced warpage for pultrusion of a rectangular hollow profile. Composites Part B: Engineering, vol. 68, p. 365–374.

21. Deng H.Y, Wang Z.Q, Wei T (2016). Study on grouting di_usion theory based on rheology of CW epoxy slurry.J. Yangtze. River. Sci. Res. Inst., 33, 121–124.

22. Cheng, P.D (2011). Study on Flow Characteristics of Viscous Time-varying Grouting Slurry in Porous Formation.Ph.D. Thesis, Shanghai University, Shanghai, China, October.

23. Zhu, X.D, Wang, L.J (2017). Analysis of rheological properties and curing properties of RTM Epoxy Resin. Fiber Reinf .Plast. Compos 8, 97–101.

24. Liu Z.F, Xiao J.Y, Zeng J.C (2008). Study on the process performance of low viscosity epoxy resin VIM. J. Natl. Univ. Def. Technol. 30, 20–24.

25. Halley, P.J.; Mackay, M.E (1996). Chemorheology of thermosets: An overview. Polym. Eng. Sci.36, 593–609.

26. Kiuna, N.; Lawrence, C.J (2002). A model for resin viscosity during cure in the resin transfer moulding process. Compos. Part A, 33, 1497–1503.

27. Zhang, W.; Duan, Y.X.; Zhao, Y. (2000). Study on low viscosity epoxy resin system for resin transfer moulding process. Polym. Mater. Sci. Eng. 2000, 16, 86–88.

28. Zhenhua S, Zaiqin W, Da Z and Tao W (2019). Study on Rheological Behavior and Surface Properties of Epoxy Resin Chemical Grouting Material Considering Time Variation, Materials 2019, 12, 3277.

29. Chang W. R, Etsion I and Bogy D. B. (1988). Static friction coefficient model for metallic rough surfaces. Journal of tribology, january, vol. 110/57.

30. Chang, W. R, Etsion, I, and Bogy, D. B., (1987). Elastic-Plastic Model for the Contact of Rough Surfaces. ASME JOURNAL OF TRIBOLOGY, Vol. 109, pp.257-263.

31. Chang, W. R, Etsion, I, and Bogy D. B. (1988). Adhesion Model for Metallic Rough Surfaces. ASME Journal of Tribiology, pp. 50-56.

32. Berger G.R, Steffel C and Friesenbichler W (2015). On the Use of Interfacial Tension Parameter to Predict Reduction of Friction by Mold Coatings in Injection Molding of Polyamide 6, Proceedings of the Regional Conference Graz – Polymer Processing Society PPS.

33. Steffel C (2014). Studies on the predictability of friction between polymers and coated / uncoated mold surfaces by wetting parameters. Master thesis, Montanuniversitaet Leoben.

34. . Berger G. R, Steffel C, Friesenbichler W (2015). A Study on the Role of Wetting Parameters on Friction in injection molding., submitted to Special Issue on "PMI: Polymers and Moulds Innovations", Int. J. of Materials and Product Technology (Inderscience Publishers.

35. Delaney K. D., Bissacco G., et al. (2012). A Structured Review and Classification of Demolding Issues and Proven Solutions. International Polymer Processing 27 (1), 77-90.

36. Tian Q L, Peng F, Yuwei W, Shuxin L, Xinmiao M (2021). Developing an innovative curved-pultruded large-scale GFRP arch beam. Composite Structures 01 Vol. 256.

37. Mukherji A, Tarapore N.D, Wakure G.N. Designing of Hybrid Structured Glass Laminated Transparent Nano Composites through Vacuum infusion Technique. MST International Journal of Chemistry, Volume 1, 1, 2016.

38. Arindam M (2017). Prediction of cure mechanism of Polyester Resin based composites across die during Pultrusion process. 4th Annual National conference " 6th Recent Advancement on Polymer Technology. National conformance Jan 27-28th India

39. Arindam M, Patil K, Tarapure N.D, Wakure G. (2017). Material configuration in the Die, influences Pultrusion process parameters and Part Properties. 6th Recent Advancement on Polymer Technology. National conformance Jan 27-28th , India

40. Arindam M, Patil S (2017). Flow behaviour of Ferro fluids and its effect on thermal conductivity. 6th Recent Advancement on Polymer Technology. National conformance Jan 27-28th , India

41. Arindam M and James N (2018). Material configuration in the die, influences pultrusion process parameters and part properties. 4th International Conference on Structural Nano Composites (NANOSTRUC2018). 23-25th May, Berlin, Germany.

42. Kirill M, Alexander V, Alexander S and Iskander A (2021). Thermoplastic Pultrusion: A Review Polymers 13, 180.

43.Renato M. B (2017). Modelling and Simulation of the Closed Injection Pultrusion Process. Dissertation of M.Sc. Karlsruher Institut für Technologie (KIT)

Caption of Figures and Tables

Tables

Figures

Figure 16: Pull-force recorded using device during pulling post curing

Figure 17: Influence of fibre volume fraction and profile thickness on compaction pressure during pulling

Figure 18: Influence of pulling speed and tapping angle on pressure due to friction during pulling

Nomenclature & Symbols

Symbols	Nomenclature	Symbols	Nomenclature
∇	pressure difference	K	permeability
V_f	fibre volume fraction.	R	Particle radius
k_c	Kozeny constant,	β	constant representing ratio of span length to span height of the fibres involved.
P	pressure normal to surface	V_0	initial fibre volume
V_a	maximum fibre volume fraction	U	pulling speed
B	transversal stiffness of fibres	$K_{(x)}$	longitudinal permeability
dP/dx	Change of Pressure difference with change in axial distance	$\Delta v/v$	resin resultant volume changes due to thermal expansion and overall shrinkage
V_{fx}	fibre volume fraction as functions.	$P(x)$	Pressure at specific axial distance
x	Axil distance	F_{com}	Force due to compression
F_{tot}	Total force	F_{vis}	Viscous Force

w	Die width	F_{fric}	Force due to Frition
$\dot{p}$	Resin injection Pressure	τ	Shear strength/stress
σ	Contact Pressure	F	Contact force of the Fibres
δ	Fibre Deflection	E	Modulus of the Fibres
L	length of the Fibre Segment	I	Inertia of Bending of the Fibres
l_0	Initial height of the prism	l_{min}	Minimal Height
$\dot{w}$	Width of the prism	$\hat{G}$	Theoritica Bulk Modulus
l	height of the prism	d	diameter of the fibre
f	Co-efficient of Friction	L_m	Length o Tapper section
h_L	Hight of flat portion of the conical die from centre	ρ_f	Density of fibres
A		N_r	Number of roving in specific volume
Φ	porosity	δP	pressure gradient
L_w	linear weight of fibre	$h(x)$	
U_x	resin flow speed	$Q_R(x)$	Relative matrix flux
$Q(x)$	volumetric flux	η_0	Initial viscosity
η_a	apparent viscosity	$\hat{\lambda}$	resin layer thickness
γ	shear rate	G	shape factor
n	dimensionless constant	P_d	Pressure due to Drag

θ	initial taping angles	P_f	Pressure due to dry friction
P_c	Pressure at Compaction	$h_{(x)}$	Hight of conical die at x
P_v	Pressure due to viscosity	r	distance between the layers or fibres
η_a	Apparent Viscosity	A_d	Adhesion load
η_v	Average viscosity	θ_f	average angle
$\hat{\dot{\theta}}$	contact angle of liquid-solid phase	S	shrinkage factor
P_{ef}	Effective Pressure due to dry friction	$\hat{\lambda}$	Time constant
δR	Shrinkage of part		

Tables

Table 1. Materials and formulation used for the friction measurement

Ortho -Polyester resin	*Mechemco*	100 phr
Perkadox-C	*Ackzonoble*	0.050 phr
MEKP	*Aldrich Chemical*	0.25–0.50 Phr
BPO	Veekay Chemicals	1.0 Phr
TBPB	Veekay Chemicals	1.2 Phr
Calcium Carbonate -400	*GULSHAN Polyols Limited*	30 pbw
Release Oil	*Fine Organics*	1 pbw

Table 2: Formulation and conversion in dead-end polymerization experiments

Initiator MEKP	0.25	0.32	0.40	0.48
Residual heat (J/g)	239	230	212	176
Conversion (%)	27	30	42	50

Table 3. Comparison between Model Fitting and Measured Values

Effects on	Tapping Angle (Radian)		Speed of Pulling (m/min)			
	0.01734	0.0163	0.2	0.25	0.35	0.45
Pull-force Measured (Max in N)	5600	4568	3200	3690	4680	6600
Model fitting - Pulling Pressure (Max in Kg/m2	6.95 $x10^4$	6.4 $x10^4$	5.89 $x10^4$	6.43 $x10^4$	--	----

Figures

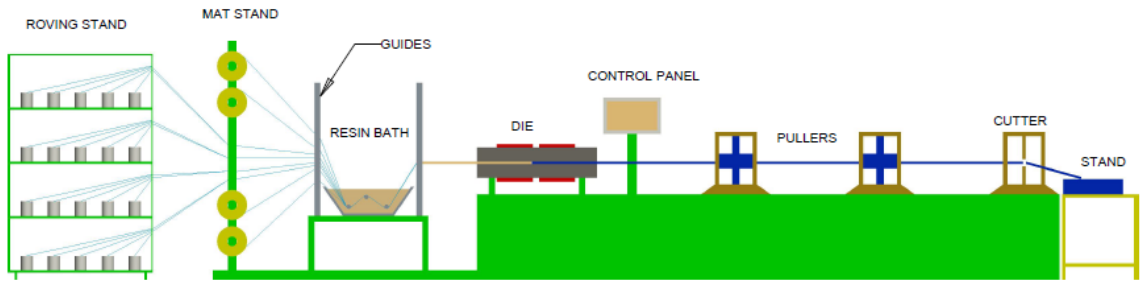

(a)

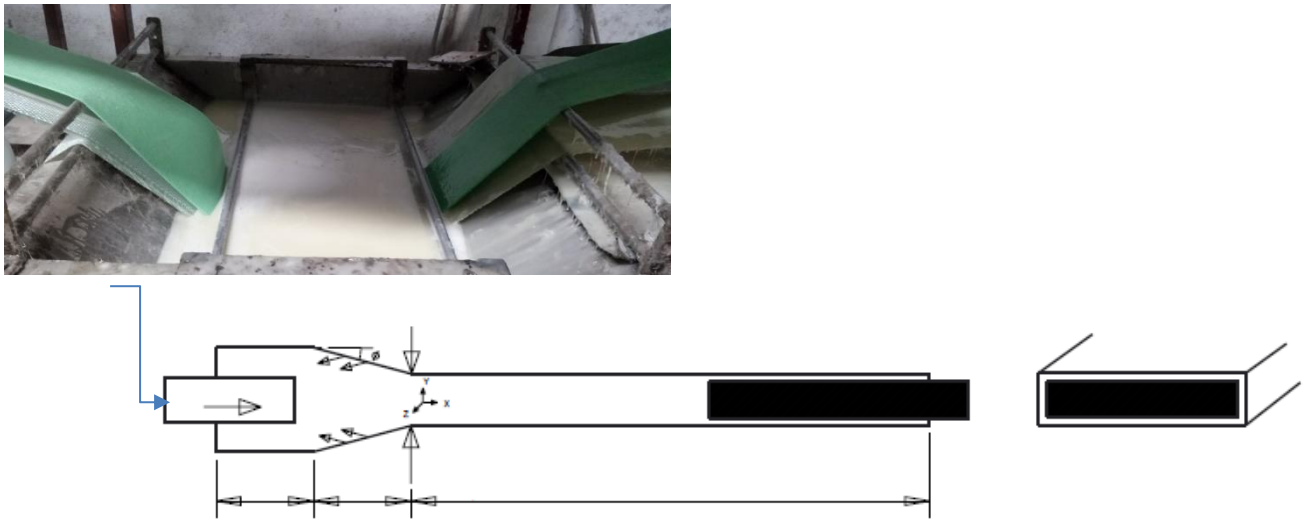

(b)

Figure 1: (a)The schematic of the open bath pultrusion line, (b) the schematic of compaction zone in conventional pultrusion die

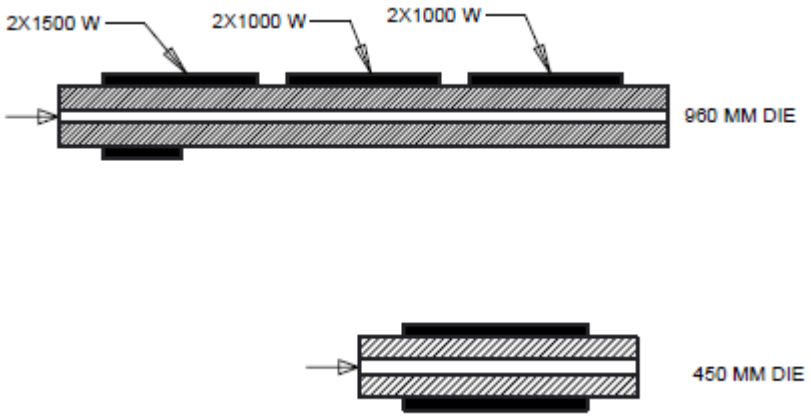

(a)

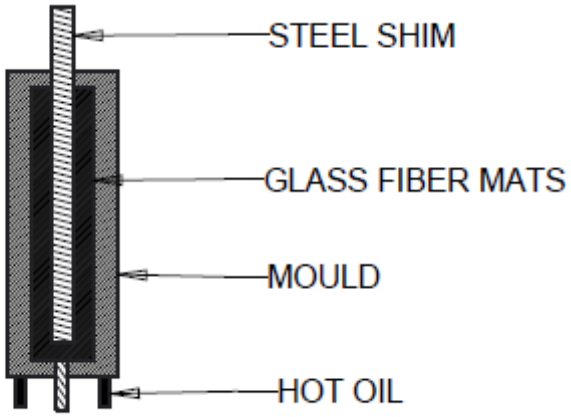

(b)

Figure 2: (a)The schematic of short straight die length, (b)the schematic of side view of the mould used to predict the pull force in liquid zone

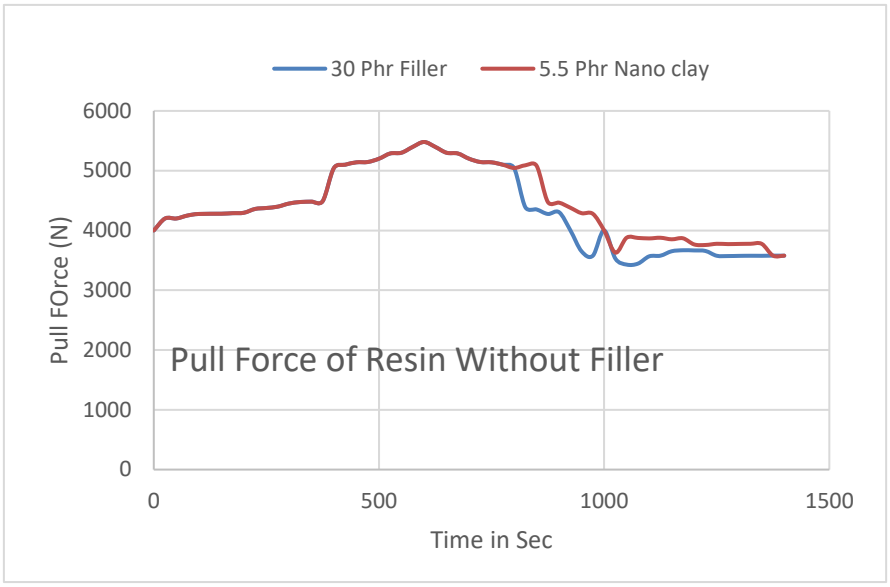

Figure 3: Measured values for change in pull force along axial length during start up pulling

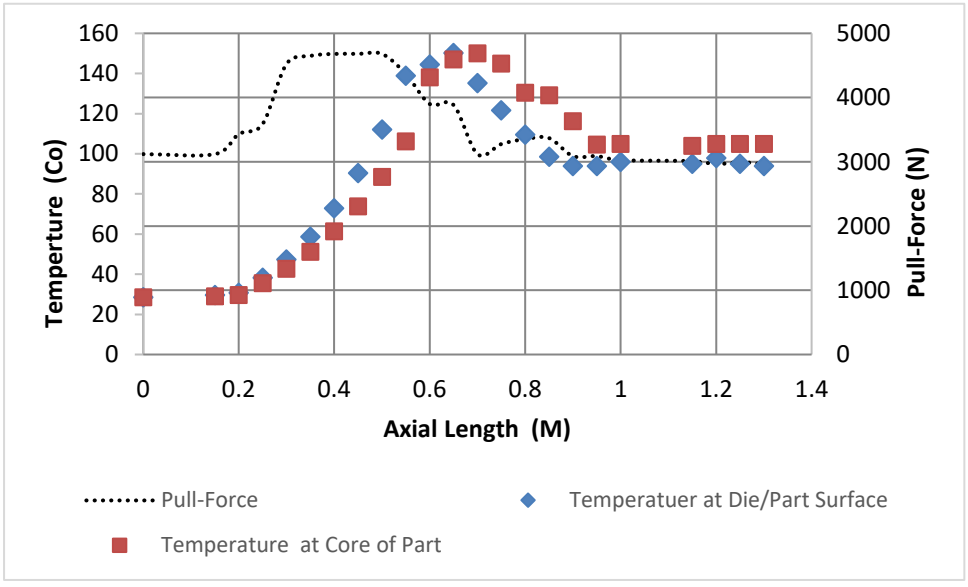

Figure 4: Measured values for changes in temperature at Core and Surface and Pull force during pulling along axial length

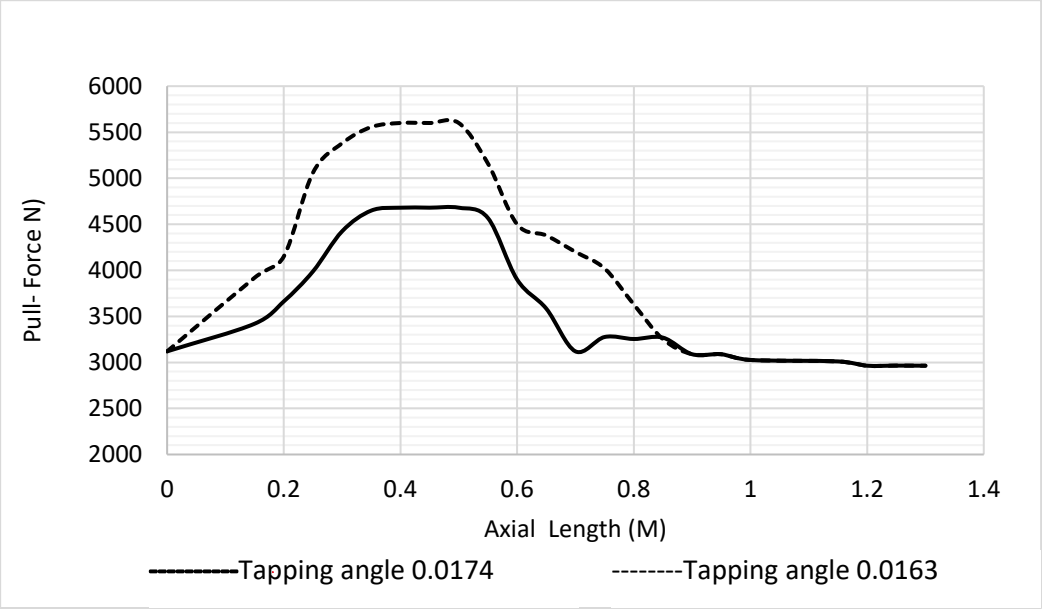

Figure 5: Measured values for changes in pull force during pulling at varying degree of compaction during pulling operation

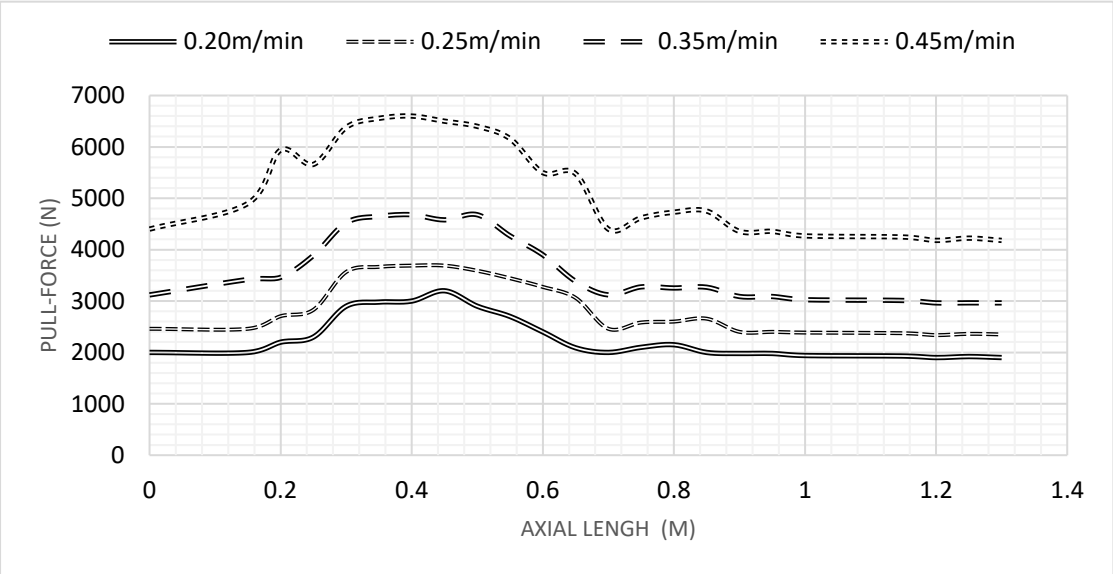

Figure 6: Measured values for changes in pull force at different experimental pulling speed along axial distance.

(a)

(b)

(c)

(d)

Figure 7: (a) Stable product in operation during pultrusion pulling, (b and c) Scaling of product in operation during pultrusion pulling (d) part failure in operation during pultrusion pulling

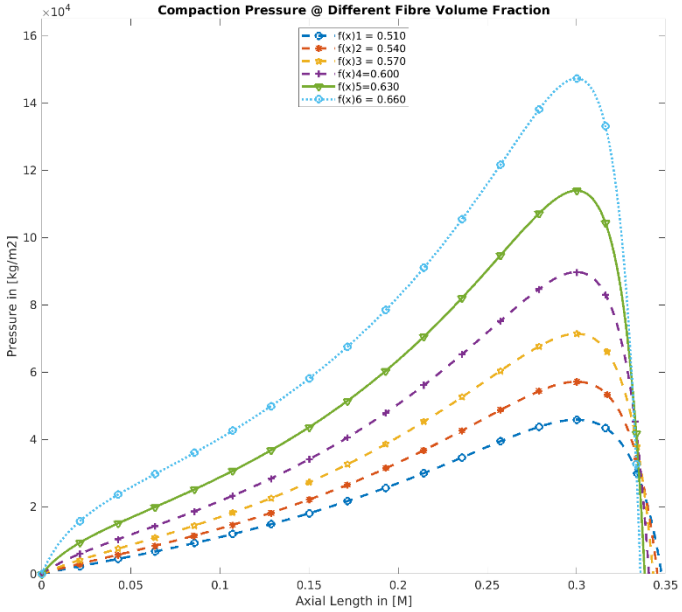

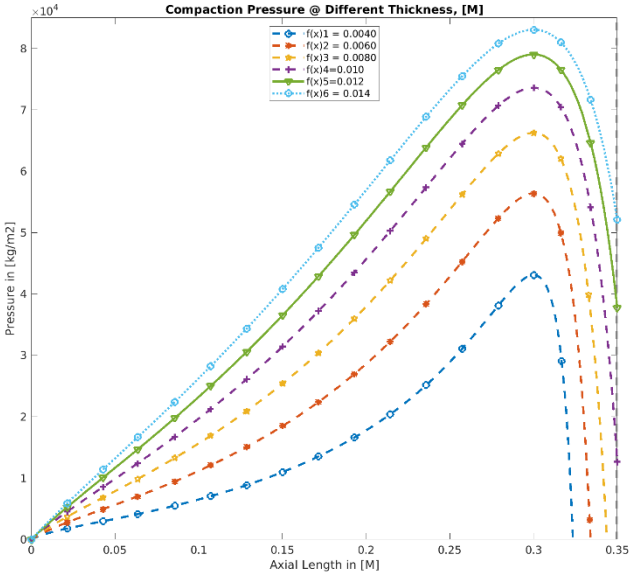

Figure 8: Experimental results showing the Influence of (a) fibre volume fraction and (b) profile thickness on compaction pressure during pulling

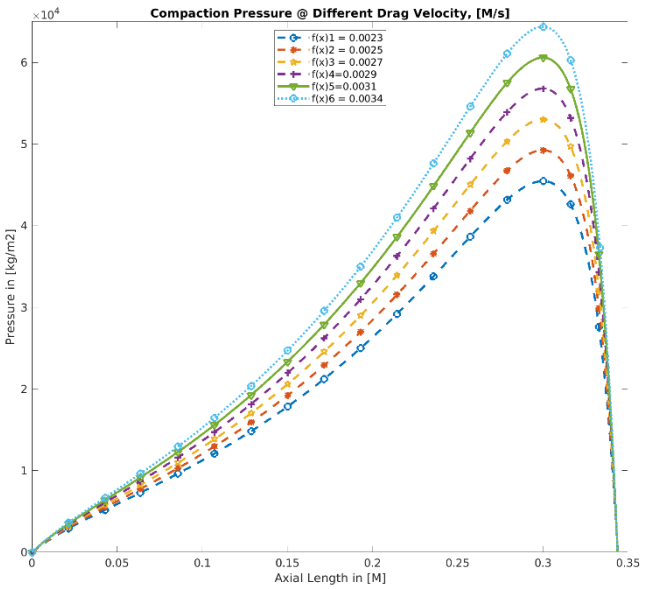

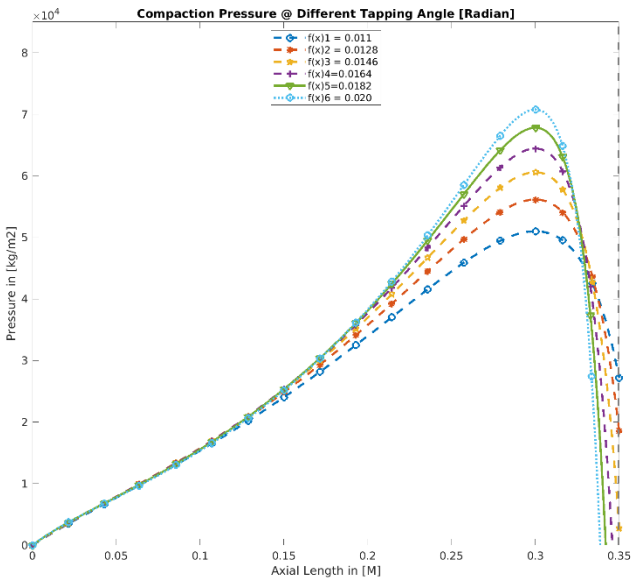

Figure 9: Experimental results on the influence of (a) pulling speed and (b)tapping angle on compaction pressure during pulling

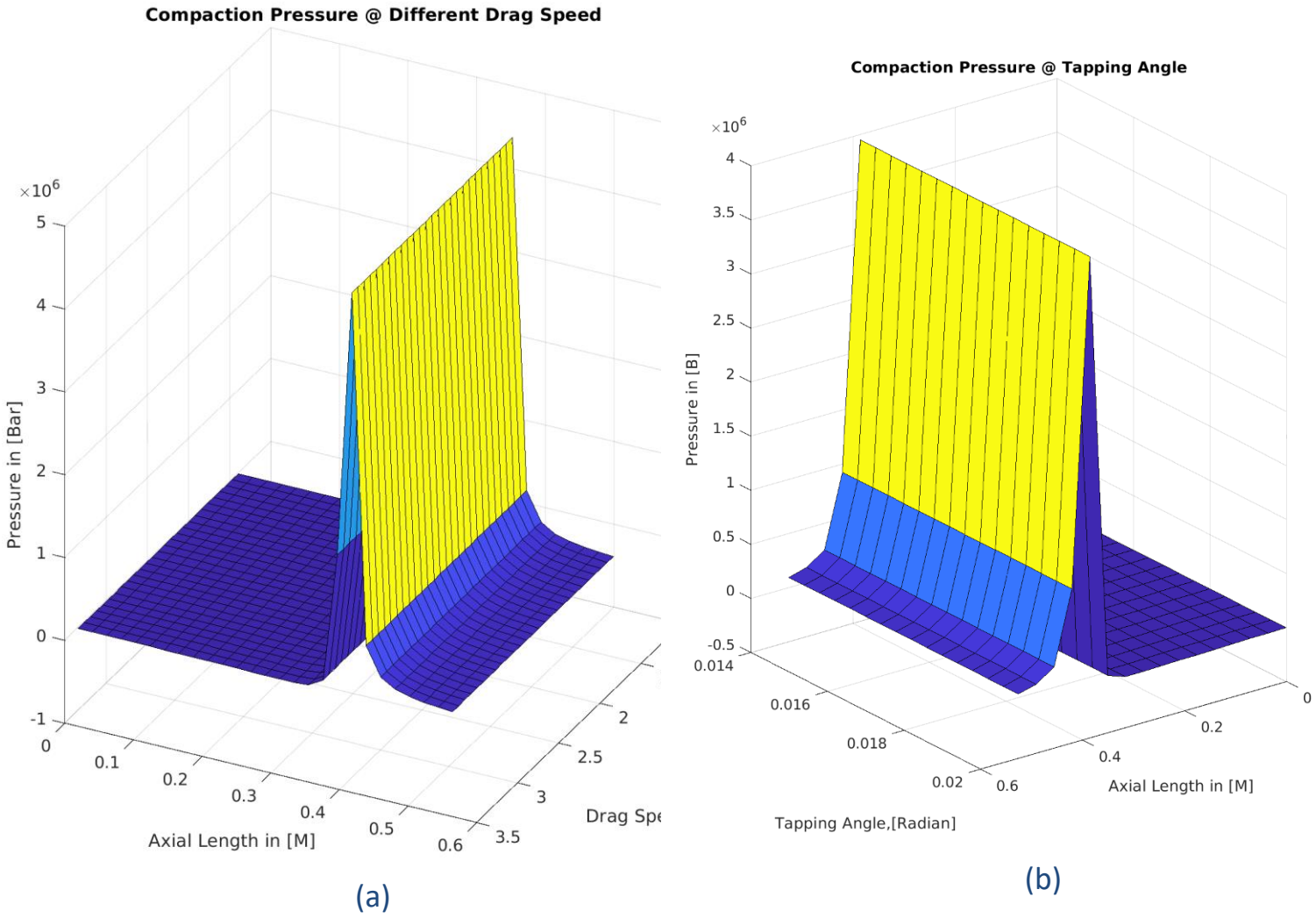

Figure 10 (a): 3-D Surface plot on influence of tapping angle on compaction pressure and (b): 3-D Surface plot on influence of profile thickness on compaction pressure

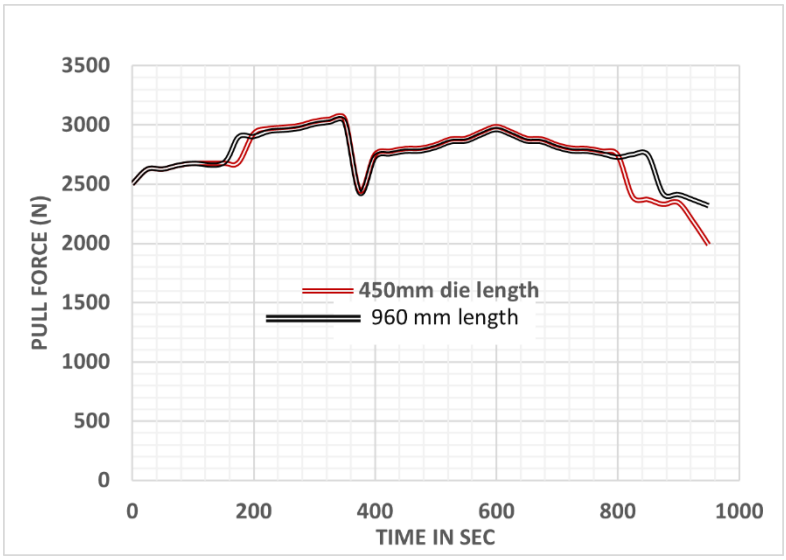

Figure 11: Effect of speed and die length during pulling in liquid zone before solidification

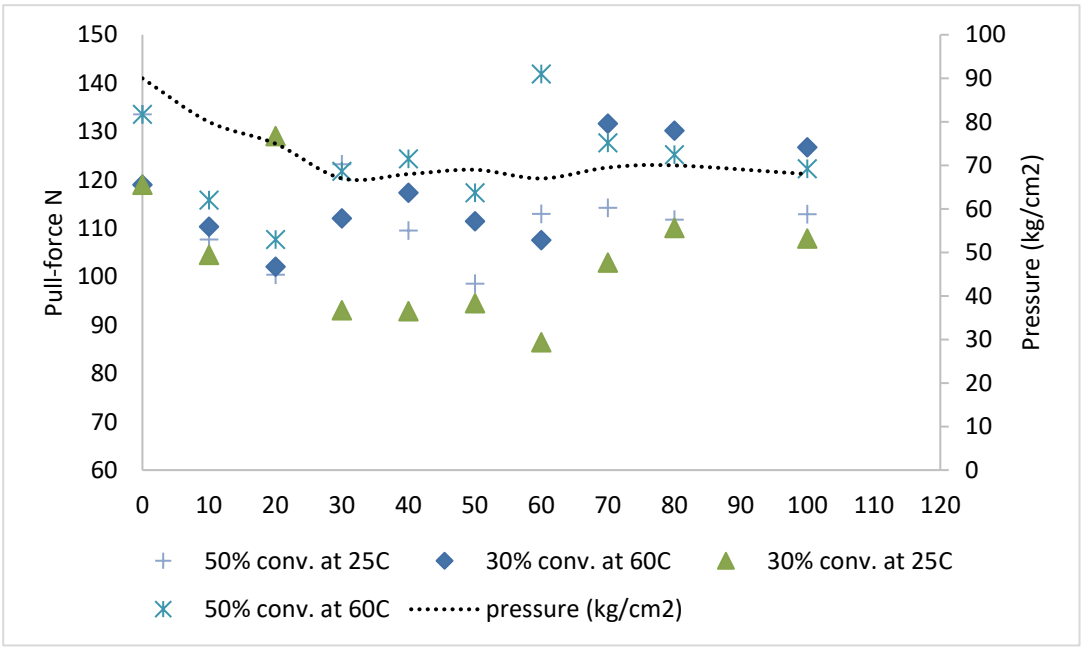

Figure 12: Pull - force recorded using device for viscous drag during pulling

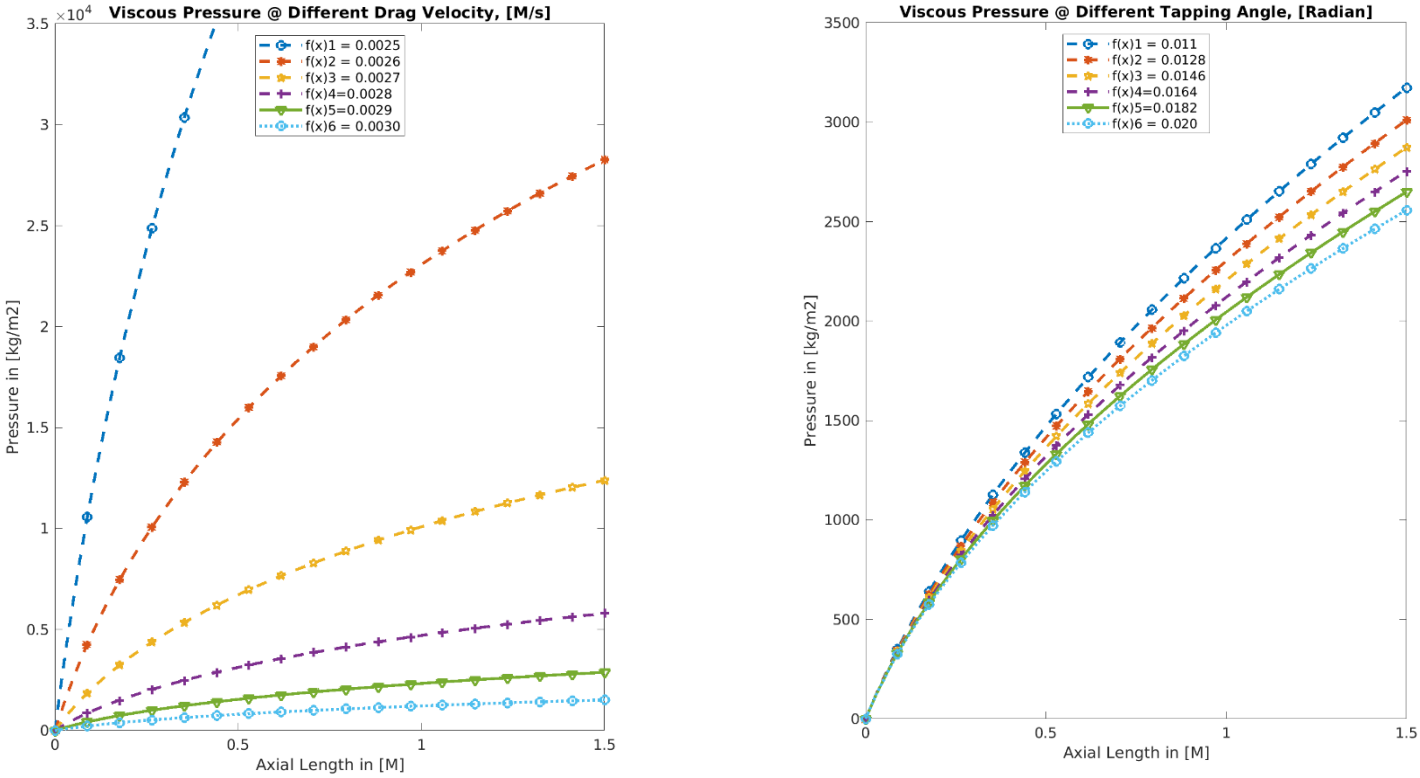

(a) (b)

Figure 13: Influence of (a)fibre volume fraction and (b) profile thickness on viscous pressure during pulling

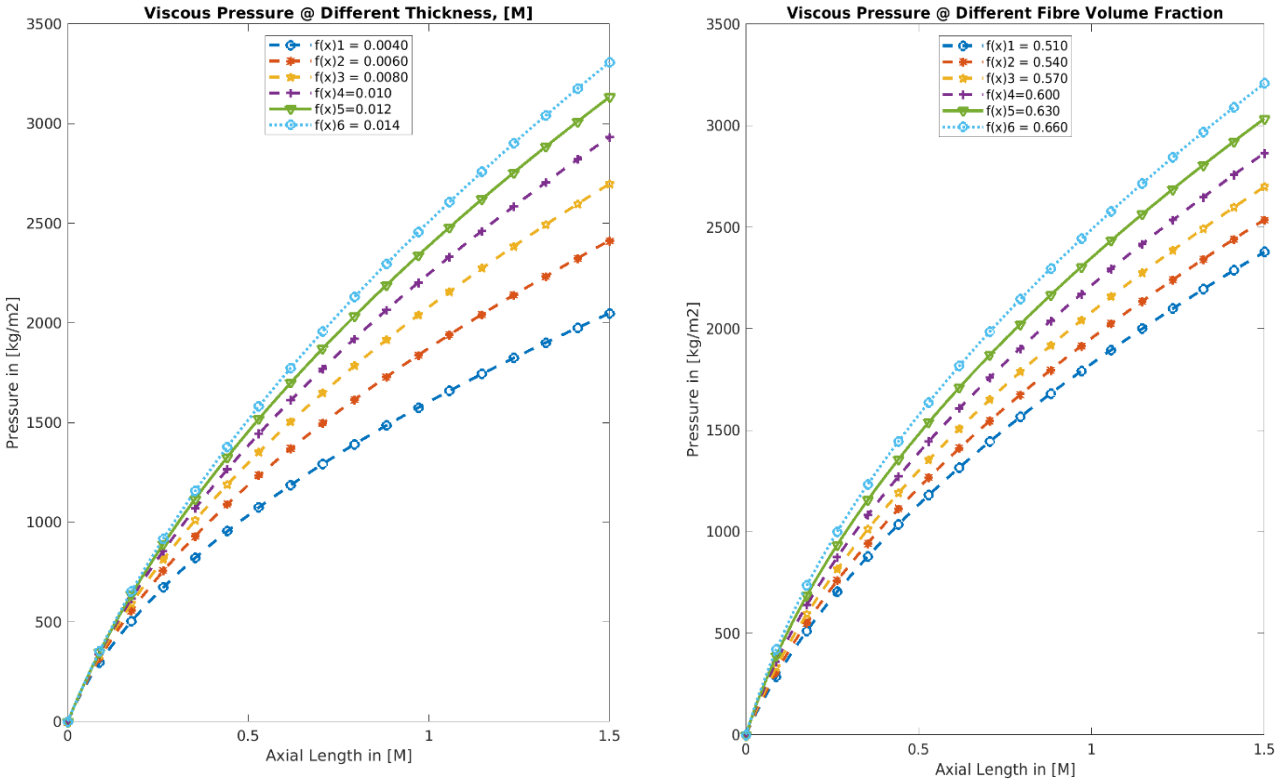

Figure 14: Influence of (a) fibre volume fraction and (b)profile thickness on viscous pressure during pulling

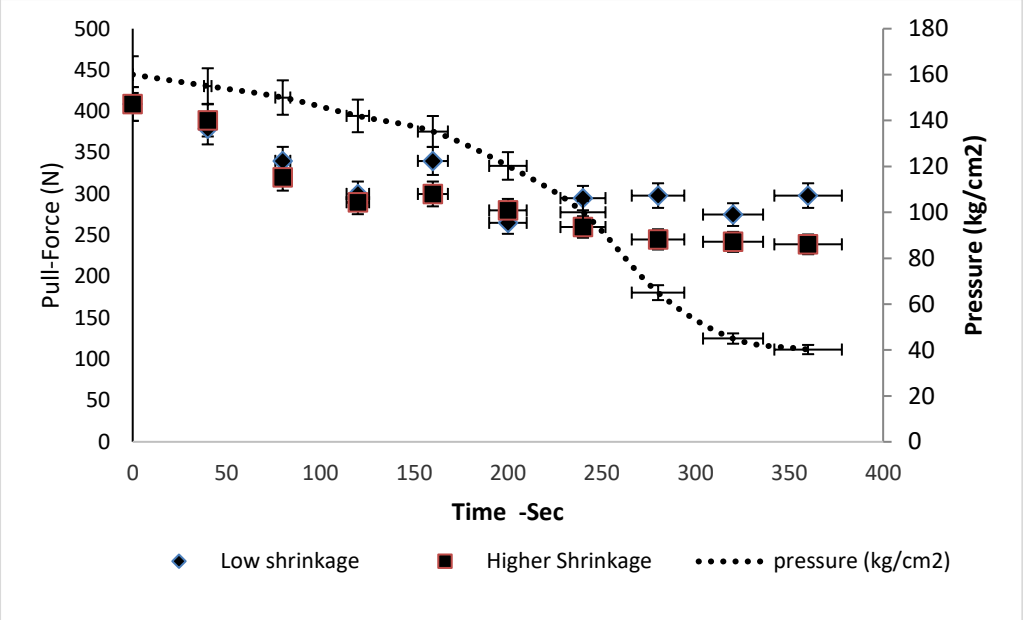

Figure 15: Pressure /pull-force recorded of polyester resin at different characteristic shrinkage

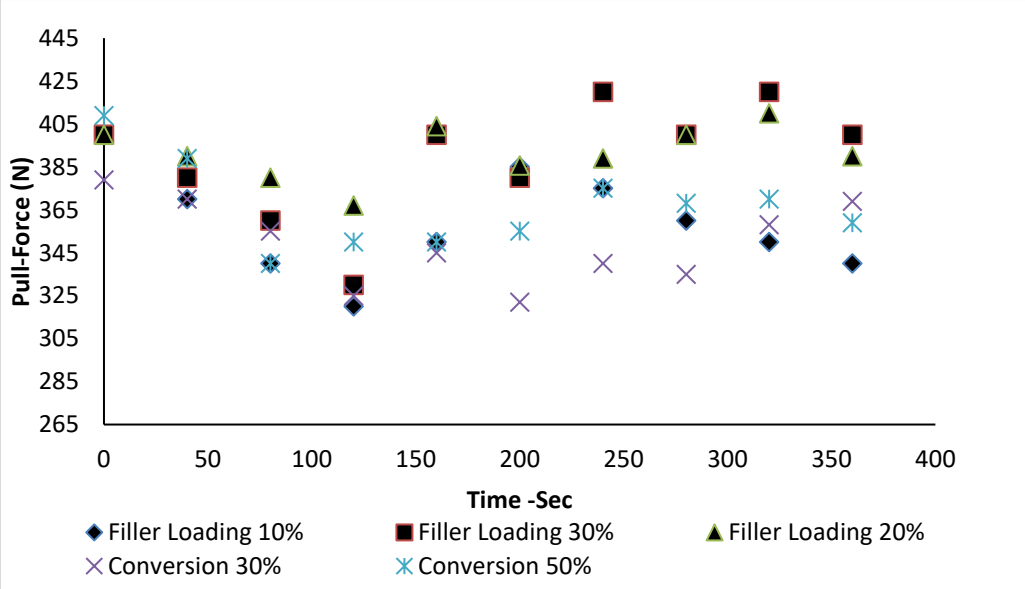

Figure 16: Pull-force recorded using device during pulling post curing

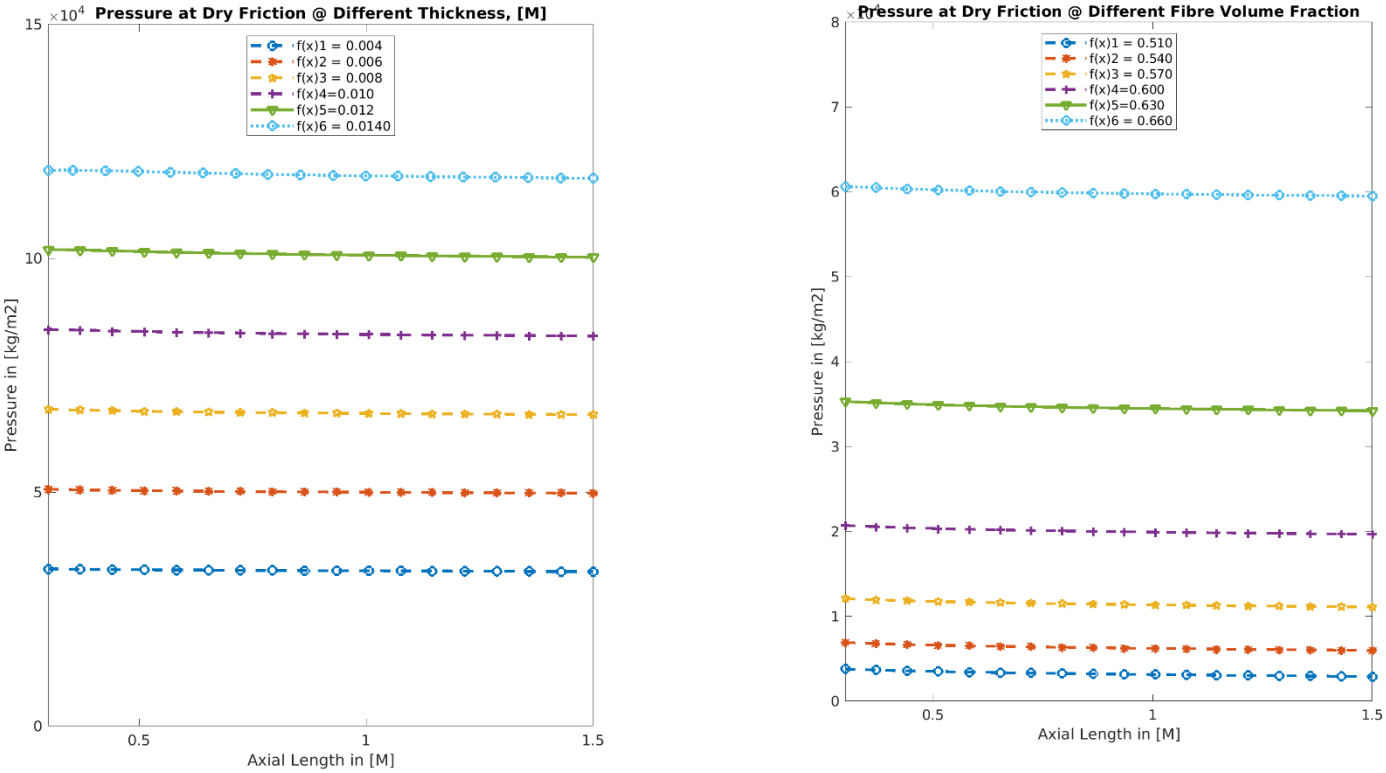

(a) (b)

Figure 17: Influence of (a)fibre volume fraction and (b)profile thickness on compaction pressure during pulling

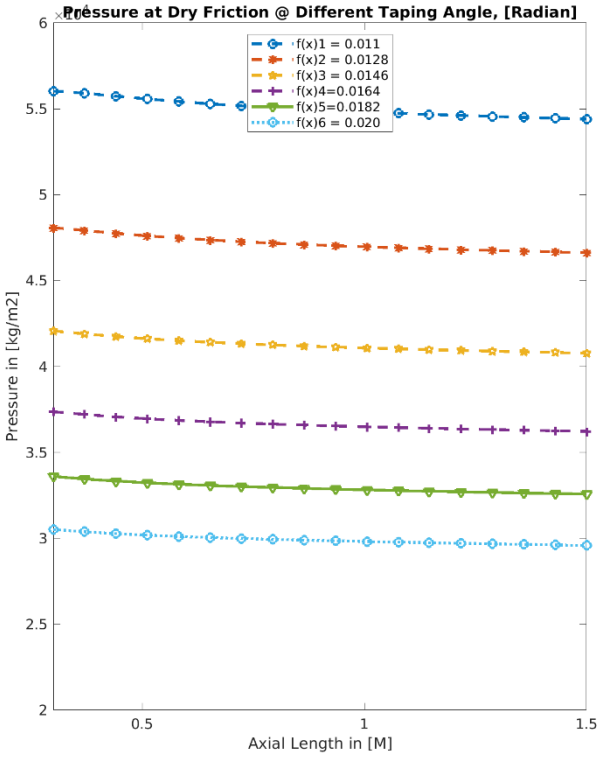

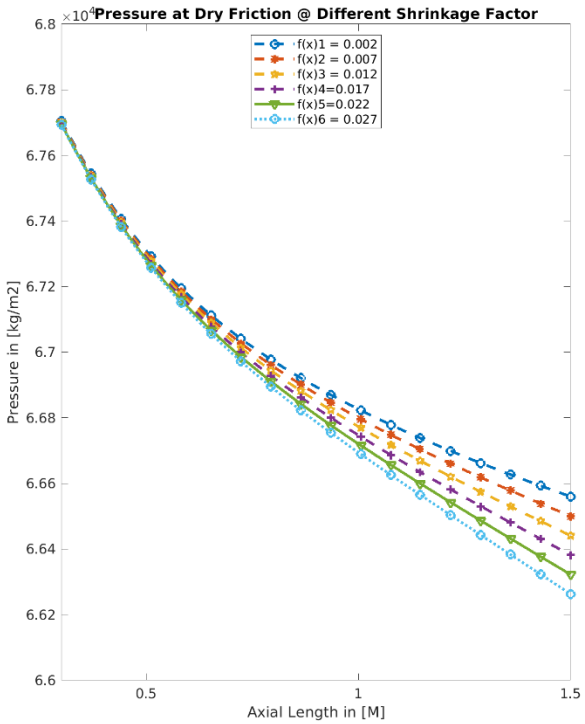

(a) (b)

Figure 18: Influence of pulling speed and tapping angle on pressure due to friction during pulling